JOURNAL OF MATERIALS SCIENCE 31 (1996) 3397–3402

Neutron diffraction texture study of deformed uranium plates

C. S. CHOI
Energetics and Warheads Division, ARDEC, Picatinny Arsenal, NJ 07806, and Reactor Radiation Division, NIST, Gaithersburg, MD 20899, USA

M. STAKER
Army Research Laboratory, Aberdeen Proving Ground, MD, USA

The texture of two depleted uranium (DU) samples, labelled DUWR and DUWR2, were studied by neutron diffraction. DUWR was prepared by warm rolling of a cast ingot, and DUWR2 was prepared by adding 20% tensile strain to the warm-rolled DUWR. Complete three-dimensional orientation distribution functions were determined using four neutron pole figures for the DUWR, and using six neutron pole figures for the DUWR2 sample, by the WIMV method of the program popLA. The textures of the two samples were essentially identical to each other. They could be described by a twisted helical density tube spiralling continuously along the ψ-axis of the Euler space. The projection of the backbone of the density tube along the θ-axis cast a linear shadow running parallel to the diagonal of the ϕ–ψ plane, which could be defined by a $\phi = \psi + 90°$ (and $\phi = \psi + 270°$) relation. The helical tube was confined within narrow θ-angle limits, from 14° to 30° with the peak orientation at (1 0 3) ⟨0 1 0⟩. The diffraction patterns of the DUWR2 sample were measured from the normal direction to the rolling surface of the sample, up to the scattering angle of 108° using a 0.15 nm neutron beam. The Rietveld profile refinement using the textured diffraction pattern was quite satisfactory when the texture effect to the entire diffraction profile was corrected for by the corresponding pole density from the inverse pole figure.

1. Introduction

Alpha-uranium, the allotropic form of uranium metal stable up to 670 °C, crystallizes in an orthorhombic *Cmcm* space group with, $a = 0.285\,38$ nm, $b = 0.587\,01$ nm, and $c = 0.495\,57$ nm [1]. Uranium is a well-known fissile material, and widely used for nuclear energy and also for nuclear weapons. It also has been used for armour-piercing weapons because it is one of the heaviest metals naturally available. Texture development in uranium has been studied extensively, but no complete three-dimensional analysis is available yet. The texture studies reported in the literature were summarized in the Metals Handbook by Chin [2], which describes the rolling texture (300–400 °C) being {1 0 3} ⟨0 1 0⟩ and the warm-rolling texture (higher than 500 °C) being (1 $\bar{4}$ 6) ⟨4 1 0⟩ + (1 0 3) ⟨0 1 0⟩.

X-ray is the most popular source used for the diffraction studies of materials including texture measurements, mainly because of the strong intensity and the easy availability. However, the X-ray method has a serious disadvantage, i.e. weak penetration power owing to the high absorption of X-rays, which causes the X-ray beam to be reflected mostly from a thin surface layer of the heavy metallic material. Texture measurements by X-rays, therefore, require a certain shape for the specimen: either a flat surface for the reflection method, or a thin plate form for the transmission method. These geometrical constraints impose an inherent limit to the measurable orientation, and produce an incomplete pole figure. Subsurface texture measurements by X-rays can be accomplished only by a destructive method for most solid materials. A neutron beam, on the other hand, has generally a much stronger penetration power for most materials. It is suitable particularly for the study of a heavy metal. For a uranium metal, the CuK_α characteristic X-ray (0.154 nm) has an absorption cross-section about 12 000 times larger than the neutron beam of the same wavelength. Specifically, the CuK_α X-ray beam loses half its intensity at a penetration distance of 1.22 μm in uranium metal. Thus, the X-ray pole figure of a uranium sample represents the texture of a surface layer a few-micrometres thick. On the other hand, the half-reduction distance of the same wavelength neutron beam is 1.47 cm in the same materials. Because the neutron beam interacts with the whole volume of the specimen at all orientations, the neutron pole figures represent a whole body texture. In this study, we chose to use the neutron diffraction method.

0022–2461

2. Experimental procedure

Two depleted uranium (DU) samples, DUWR and DUWR2, were prepared for the texture study. Sample DUWR was prepared by a warm rolling of cast ingot; sample DUWR2 was prepared by applying 20% tensile strain to the warm-rolled sample (DUWR). Each sample was cut into two equal-sized pieces (19 mm × 19 mm × 2.5 mm). The two pieces were stacked together to double the sample thickness without disturbing their mutual orientation relationship.

The four-circle single-crystal neutron diffractometer at the research reactor of the National Institute of Standards and Technology, was used for the texture measurements. Each sample was mounted on the χ-circle cradle of the four-circle diffractometer, with the sample oriented with the normal direction (ND) to the sample surface parallel to the sample rotation axis (Φ-axis) of the diffractometer. Four pole figures, (0 2 0), (1 1 1), (1 1 2), and (1 3 1), were measured for the DUWR sample, and six pole figures, (1 1 0) and (0 0 1) in addition to the above four, for the DUWR2 sample. The intensity distribution was measured over the entire orientation hemisphere, with the χ-angles ranging from 90°–0° and Φ-angles from 0°–360°, each with 5° step intervals, using 0.1275 nm wavelength neutrons. The background intensities were measured at off-Bragg positions in each χ-angle orientation. Absorption corrections were made by assuming that the linear absorption coefficient of uranium metal is about 0.47 cm^{-1}. The corrected intensities were converted to the pole density in the unit of the multiples of the random distribution (mrd), by normalizing the observed intensities to the calculated powder diffraction intensity using routine procedures [3]. The four experimental pole figures of DUWR are presented in Fig. 1, and those of DUWR2 are shown in Fig. 2. The

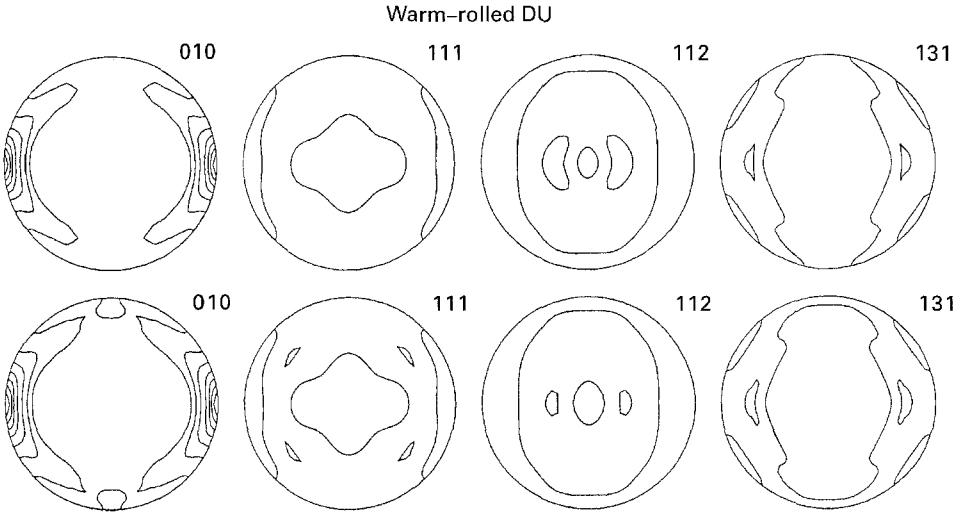

Maximum = 8.11; minimum = 0.00; contour(1) = 1.00; contour(2) = 2.00; contour(3) = 3.00; etc.

Figure 1 The experimental pole figures (top), 0 1 0, 1 1 1, 1 1 2, 1 3 1, and the corresponding recalculated pole figures (bottom) of the DUWR sample, presented with the equal-area type projection. The contour levels of 1 mrd and higher are given in 1 mrd steps.

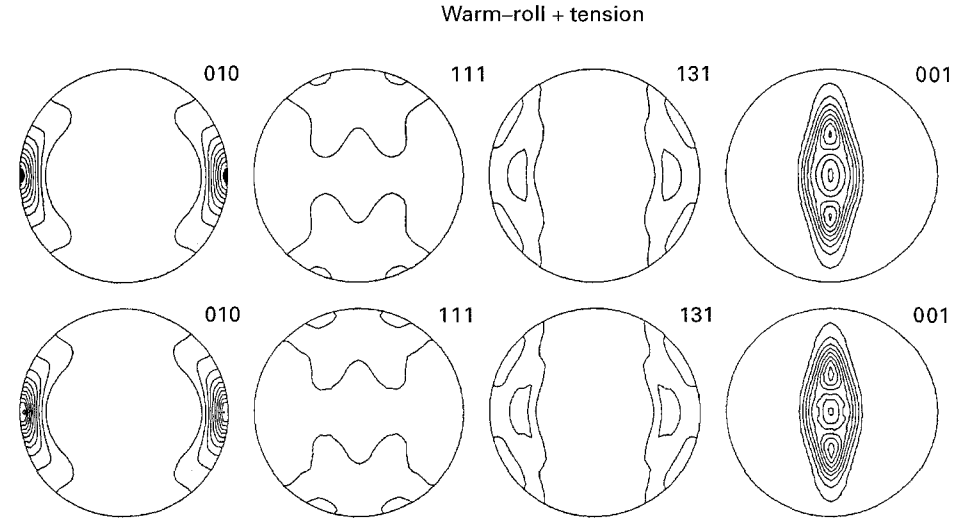

Maximum = 11.39; minimum = 0.00; contour(1) = 1.00; contour(2) = 2.00; contour(3) = 3.00; etc.

Figure 2 The experimental pole figures (top), 0 1 0, 1 1 1, 1 3 1 and 0 0 1, and corresponding recalculated pole figures (bottom) of the DUWR2 sample, presented with the equal-area type projection. The contour levels of 1 mrd and higher are given in 1 mrd steps.

pole density distributions of the two samples were found to be very similar to each other.

3. Results

3.1. Orientation distribution function of DUWR

The orientation distribution function (ODF) of DUWR was analysed from the four pole figures, (0 1 0), (1 1 1), (1 1 2) and (1 3 1), by the WIMV method using the program popLA [4], imposing orthorhombic symmetry to the pole figures. After 30 cycles of iterative calculations, the RP factor (a residual parameter defined by Matties *et al.* [5]) reduced to 1.3%, and the final texture strength (square-root of the texture index [6]) reached 2.3. The recalculated pole figures obtained from the ODF showed an excellent agreement with the experimental ones, as compared in Fig. 1. The three-dimensional crystallite orientation distribution in reciprocal space (i.e. the orientation distribution of the NDs in the crystal system), commonly called SOD, is presented in Fig. 3 in constant ψ-sections ranging from $\psi = 0°$–$90°$ with 15° steps. The Kocks-type Euler angles [7] (i.e. ψ, θ and ϕ) were used for the ODF throughout.

The positions of the ND density peak in the constant ψ-level changed systematically with the increase of the ψ-angles. This implies that the preferential orientation distributions in the Euler space (called density skeleton hereafter) have a helical tube form spiralling around the [0 0 1] axis. The peak positions of the density skeleton were determined at seven different ψ-levels, from $\psi = 0°$–$90°$ with 15° steps, and are given in Table I. The peak positions in Euler angles were converted to the conventional $(h\,k\,l)$ $[u\,v\,w]$ type orientation with the orientation matrix [7], using the nearest low Miller indices, and were included in Table I. The Miller indices $(h\,k\,l)$ were calculated from the two Euler angles (θ and ϕ), and the $[u\,v\,w]$ from the three Euler angles (ψ, θ and ϕ), where ψ corresponds to the peak position in the ψ-angular distribution passing through each (θ, ϕ) peak of the SOD, as shown in Fig. 4.

3.2 ODF of DUWR2

The ODF of DUWR2 was also analysed by the WIMV method, using six pole figures, (0 1 0) (1 1 1) (1 1 2) (1 3 1) (1 1 0) and (0 0 1), imposing the orthorhombic sample symmetry. Among the six pole figures,

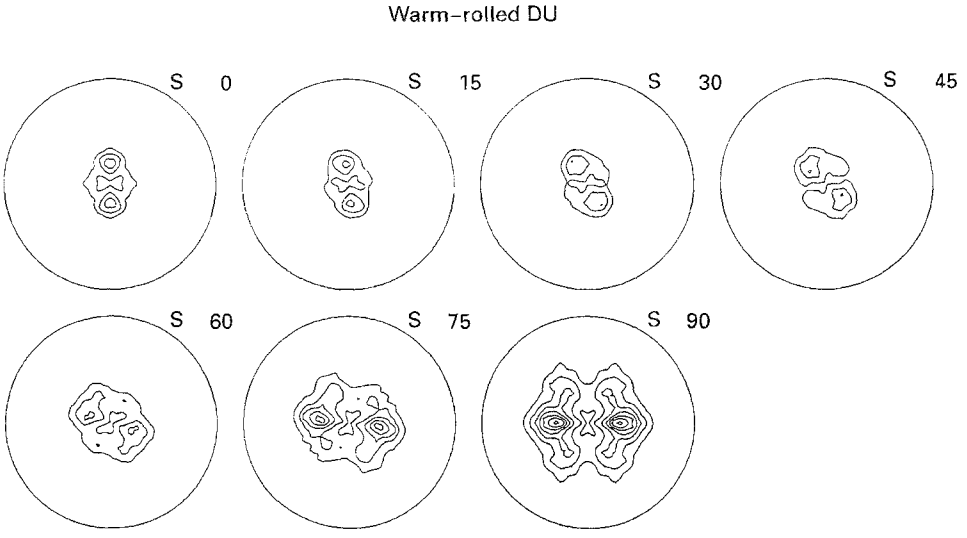

Figure 3 The sample orientation distributions (SOD) of the DUWR sample, presented in constant ψ sections, from $\psi = 0$–$90°$ with 15° steps, using the Kocks-type Euler angles. The contour levels of 3 mrd and higher are given in 3 mrd steps.

TABLE I The strongest orientation found in each ψ level of the SOD is presented in $(h\,k\,l)$ $[u\,v\,w]$ form, for the ψ-angle from 0°–90° in 15° steps. All peak positions were constrained approximately by the relation of $\phi = \psi + 90°$, and the θ-angles near $\theta = 15°$ for most of the ψ-ranges except $\psi = 90°$ where the (1 0 3) [0 1 0] texture prevailed

$(h\,k\,l)$ $[u\,v\,w]$	ψ	θ	ϕ	Density (WR2)	Density (WR)
(0 1 3) [0 $\bar{4}$ 1]	0	16	90	16	11
($\bar{1}$ 7 24) [0 $\bar{5}$ 1]	15	14	106	14	9
($\bar{1}$ 3 12) [0 1 $\bar{1}$ 2]	30	14	124	13	8
($\bar{3}$ 5 24) [0 $\bar{6}$ 1]	45	16	141	13	9
($\bar{1}$ 1 7) [0 1 $\bar{0}$ 1]	60	15	154	14	9
($\bar{2}$ 1 13) [0 1 $\bar{7}$ 1]	75	15	166	14	11
($\bar{1}$ 0 3) [0 $\bar{1}$ 0]	90	30	180	32	19

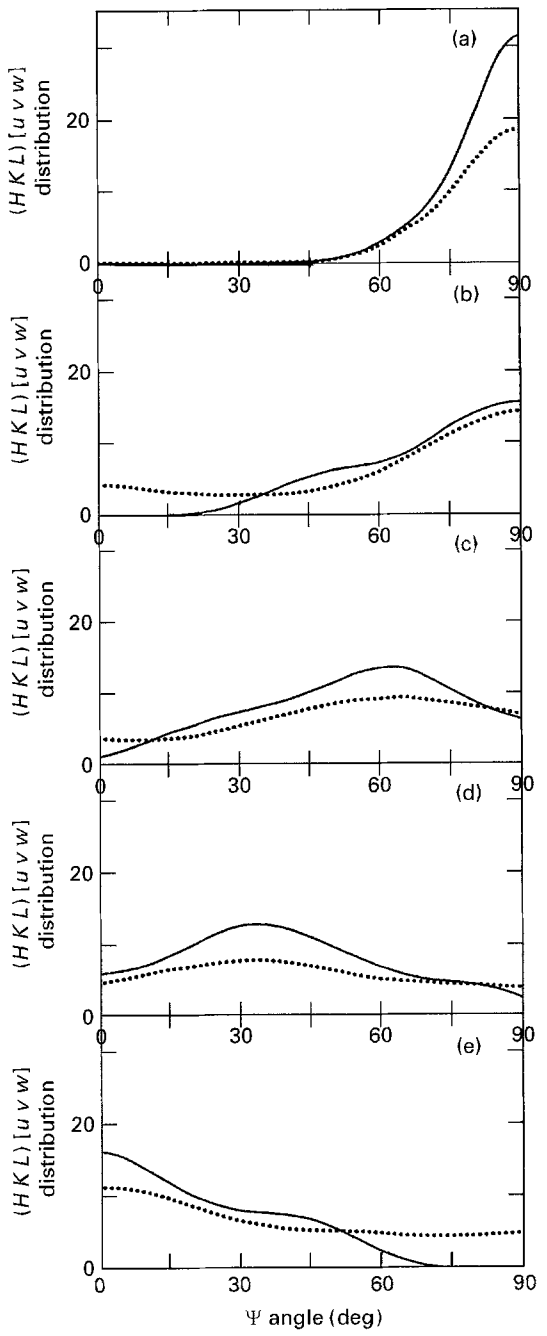

Figure 4 The $(H\,K\,L)$ $[u\,v\,w]$ distributions as a function of ψ-angles, where $(H\,K\,L)$ represents the highest intensity peak at the ψ-section of $\psi = 0°$, 30°, 60°, and 90°. (—) The density (mrd) for the DUWR2, (···) the density for the DUWR sample. (a) $(\bar{1}\,0\,3)$ $[u\,v\,w]$, peak $(\bar{1}\,0\,3)$ $[0\,-1\,0]$; (b) $(\bar{1}\,0\,6)$ $[u\,v\,w]$, peak $(\bar{1}\,0\,6)$ $[0\,\bar{1}\,0]$; (c) $(\bar{1}\,1\,7)$ $[u\,v\,w]$, peak $(\bar{1}\,1\,7)$ $[0\,-1\,0\,1]$; (d) $(\bar{1}\,3\,12)$ $[u\,v\,w]$, peak $(\bar{1}\,3\,12)$ $[0\,1\,\bar{1}\,2]$; (e) $(0\,1\,3)$ $[u\,v\,w]$, peak $(0\,1\,3)$ $[0\,\bar{4}\,1]$.

(1 1 0) and (0 0 1) may contain some systematic errors, because the diffraction peaks were not sufficiently separated from the adjacent strong (0 2 1) peak. After 30 cycles of iterative calculations, the RP error reduced to 1.7%, with a texture strength of 2.5, which is about 0.2 higher than that of the DUWR sample. This indicates that the DUWR2 sample has a stronger texture than the DUWR sample. Four of the six experimental pole figures were compared with the corresponding recalculated ones in Fig. 2. The agreement between the experimental and the recalculated pole figures is excellent. The three-dimensional SOD of the DUWR2 sample, as shown in Fig. 5, also exhibited the helical-shaped density skeleton, which was essentially identical to that of DUWR, except that the DUWR2 had considerably sharper texture with higher density. The $(h\,k\,l)$ $[u\,v\,w]$ values, as compared in Table I, are also identical to those of the DUWR. It was clear from the table that the DUWR2 sample had clearly stronger texture than DUWR. The maximum density in the skeleton was observed at the (1 0 3) ⟨0 1 0⟩ orientations in both samples, which corresponds to 32 mrd for the DUWR2 and 19 mrd for the DUWR sample. The ψ-angular distributions passing through the peak position at the five different ψ-levels, $(\bar{1}\,0\,3)$, $(\bar{1}\,0\,6)$, $(\bar{1}\,1\,7)$, $(\bar{1}\,3\,12)$ and $(0\,1\,3)$, are presented as solid curves in Fig. 4.

3.3. Orientation density skeletons

The orientation density skeletons found in DUWR and DUWR2 are compared in Table I. The backbones of the skeletons of both samples were confined within a narrow θ-angle ranges, limited between $\theta = 14°$ and 30°, and extended along the diagonal directions of the ψ–ϕ planes, with the $\phi = \psi + 90°$ relation. The ψ–ϕ relationship implies that the $[u\,v\,w]$ direction (i.e. the RD direction) of the skeletons are restricted to the $[0\,k\,l]$ zone of reciprocal space. The envelope of the density skeletons, for example the area enclosed by the 3 mrd contour lines in the two SOD maps (Figs 1 and 5), changed their sizes gradually as a function of ψ angles, from the smallest size at 0° and 180° to the largest at 90° and 270°. The constant-ψ cross-sections of the skeleton become a true *mmm* mirror symmetric shape at $\psi = 0°$, 90°, 180° and 270°, with the mirror planes parallel to the three faces of the orthorhombic unit cell. The strongest density within each skeleton was observed at the $\psi = 90°$ and 270°, which corresponds to the (1 0 3) ⟨0 1 0⟩ orientation, as shown in Table I. The orientation of the smallest envelope observed at $\psi = 0°$ and 180° corresponds to (0 1 3) $\langle 0\,\bar{4}\,1\rangle$ orientation.

This density skeleton shape implies that the great majority of the crystallites in the samples are oriented preferentially with the ND directions tilted approximately 15° from the [0 0 1] axis, with the great majority of the RDs oriented in the $[0\,k\,l]$ direction of the crystal, as indicated by the relation $\phi = \psi + 90°$. The ND orientations were concentrated most heavily in the vicinity of the $\psi = 90°$ and 270° planes of the SOD, where the highest density orientations were {1 0 3} ⟨0 1 0⟩ type with a peak density of about 32 mrd.

3.4. Texture effect on the diffraction pattern

Samples with a low crystal symmetry, such as orthorhombic, require many pole figures for an accurate ODF determination. Because the diffractometer used for the pole figure measurements had rather low instrumental resolution, most of the peaks in the diffraction pattern were overlapped heavily, except the four peaks, (0 1 0) (1 1 1) (1 1 2) and (1 3 1), which had sufficient peak separation and intensity for the pole figure measurement. To increase the number of pole figures,

two additional pole figures, (1 1 0) and (0 0 2), which had strong intensity but overlapped partially with the adjacent strong peak (0 2 1), were measured for the DUWR2 sample. The accuracy of the ODF can be evaluated independently, by comparing the texture effect on the diffraction pattern with the corresponding inverse pole figure of the sample. If the ODF obtained from the six pole figures represents the true crystallite orientation distribution of the sample, the pole density distribution of the inverse pole figure (obtained from the ODF) should agree with the intensity variations in the diffraction pattern.

The ND inverse pole figure represents the orientation density of all the (hkl) planes oriented in the ND direction. Because the pole density at a given hkl position in the ND inverse pole figure is equivalent to the volume fraction of the (hkl) planes oriented in the ND direction, the intensities of the (hkl) reflections in the ND diffraction pattern should be proportional to the hkl pole density in the ND inverse pole figure. The hkl pole densities obtained from the ND inverse pole figure of the DUWR2 sample are summarized in Table II. Table II indicates clearly that the crystallite orientation distribution in the ND direction is extremely anisotropic. For example, the pole densities of (1 3 0) and (1 5 0) are less than 10% of the random-orientation density, and those of (1 1 5) and (0 2 5) are more than four times of the random-orientation density.

The diffraction patterns of the DUWR2 sample were measured from the ND direction (the ND direction oriented parallel to the scattering vector), up to a scattering angle of 108° using a 0.15 nm neutron beam. The observed diffraction profile agreed quite satisfactorily with the calculated Rietveld profile when the pole densities from the ND inverse pole figure (as shown in Table II) were assumed to be the volume fraction of the corresponding (hkl) reflection, by using the modified version of the Rietveld refinement program [8]. The observed and calculated patterns agreed quite well, as compared in Fig. 6. This indicates that the ND inverse pole figure (and hence the ODF obtained from the six pole figures) represents accurately the true crystallite orientation distribution in the ND direction of the sample. The unit cell

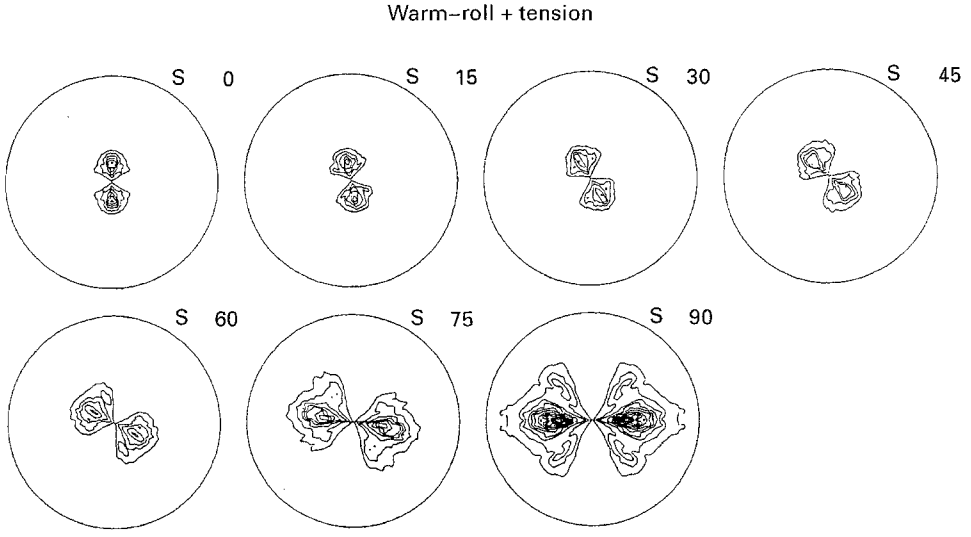

Figure 5 The SOD of the DUWR2 sample, presented in constant ψ-sections, from $\psi = 0°$–$90°$ in 15° steps, using the Kocks-type Euler angles. The contour levels of 3 mrd and higher are given in 3 mrd steps.

TABLE II The pole densities of (hkl) poles obtained from the ND inverse pole figure (mrd units). The pole density (mrd units) corresponds to the volume fractions of the (hkl) pole oriented parallel to the ND direction

(hkl)	Density (mrd)	(hkl)	Density (mrd)	(hkl)	Density (mrd)
020	0.16	110	0.16	021	0.10
002	2.92	111	0.28	022	0.23
112	1.18	130	0.04	131	0.14
040	0.16	023	1.07	200	0.29
041	0.11	113	2.73	132	0.38
220	0.16	042	0.10	221	0.20
202	0.67	004	2.92	133	0.69
222	0.28	024	2.81	114	3.91
043	0.14	150	0.06	151	0.08
240	0.07	223	0.58	241	0.11
152	0.16	134	1.12	060	0.16
061	0.12	242	0.21	044	0.23
310	0.29	025	4.20	204	2.88
311	0.33	115	4.55	062	0.11

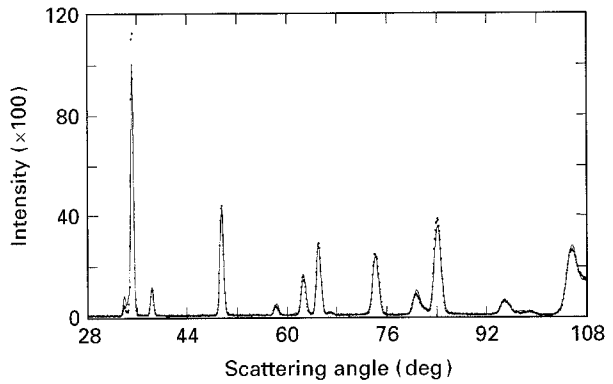

Figure 6 The neutron diffraction pattern of the DUWR2 sample measured from the ND direction. (•) Experimental data, (—) the recalculated pattern corrected for the texture effect, based on the pole density of the ND inverse pole figure.

TABLE III The final least-squares parameters of the Rietveld profile refinement of the DUWR2 sample. The unit cell dimensions (a, b, and c) are given in nm, and the half-width parameters (U, V, and W) are in squared-degree units. The position of the U-atom, $x\,y\,z$, in the asymmetric unit of the space group *Cmcm*, is given in fractions of the coordinate

$a = 0.287\,17\ (6)$	nm
$b = 0.588\,57\ (19)$	nm
$c = 0.497\,28\ (6)$	nm
$x = 0.0$	
$y = 0.1023\ (5)$	
$z = 0.25$	
$U = 2.4\ (2)$	deg^2
$V = -0.61\ (5)$	deg^2
$W = 0.14\ (1)$	deg^2

dimensions, the structural parameters, and the half-width parameters, obtained from the Rietveld profile refinement are given in Table III. The unit cell sizes obtained from the refinement were slightly larger than those reported in the literature [1], which suggests that the wavelength used in this experiment was closer to 0.1494 nm than 0.15 nm. The atomic coordinates agreed with the values reported in the literature within a standard deviation.

4. Discussion

Because the two samples exhibited essentially identical texture, as discussed above, the SOD of the DUWR2 sample is used as representative of the two textures. The preferred orientation distribution of the DUWR2 may be described as a helical tube spiralling around the ψ-axis continuously in the three-dimensional Euler space. The projection of the skeleton along the θ-axis is positioned on the diagonal of the ϕ–ψ plane, as defined by the $\phi = \psi + 90°$ (and $\phi = \psi + 270°$) relation. The helical tube is confined within a narrow θ-angle range, ranging from 14°–16° over most of the ψ-range, with the peak orientation at $\{1\,0\,3\}\ \langle 0\,1\,0\rangle$. Considering the fabrication history of the two samples, that the DUWR2 sample has added 20% tensile deformation to the warm-rolled plate (DUWR), together with the close similarity between the two textures, it is conceivable that the deformation by tension and that by warm-rolling in the DU sample are produced by a very similar slip system.

The peak orientation within the helical density tube, $\{1\,0\,3\}\ \langle 0\,1\,0\rangle$, agrees with the sheet-type orientation reported in the literature. However, $(1\,\bar{4}\,6)\ \langle 4\,1\,0\rangle$ orientation for the warm-rolled uranium reported in the *Metals Handbook* [2], was found to be in error. The two poles, $(1\,\bar{4}\,6)$ representing the ND and $\langle 4\,1\,0\rangle$ representing the RD, are not orthogonal to each other in the orthorhombic unit cell of α-uranium. There is a secondary peak within the density tube, located near the $(1\,\bar{3}\,6)\ \langle 2\,3\,0\rangle$ orientation, with the peak density of 9.2 mrd for DUWR and 7.9 mrd for DUWR2. It is interesting to notice that the height of the secondary peak is higher for the DUWR than the DUWR2 sample.

The ψ-angular distributions of the orientation densities of the two samples in Fig. 4, indicated that the warm-rolled sample (dotted lines) had mostly a fibre-type texture, except the region near $\psi = 90°$. On the other hand, the tension sample (solid lines) exhibited stronger sheet-type texture, with weaker fibre-type texture. The solid lines in Fig. 4 appeared to show weak secondary peaks, as indicated by the hump at the ψ-angles near 45°, 75°, 15°, and 45° for the $(0\,1\,3)$ $[u\,v\,w]$, $(\bar{1}\,3\,12)$ $[u\,v\,w]$, $(\bar{1}\,1\,7)$ $[u\,v\,w]$, and $(\bar{1}\,0\,6)$ $[u\,v\,w]$ distribution, respectively. These secondary peaks correspond to the RD orientation at the $[2\,\bar{4}\,1]$ direction. This implies that the DUWR2 sample is developing a weak secondary density tube running through $\{0\,1\,3\}\ \langle 2\,\bar{4}\,1\rangle$, $\{\bar{1}\,3\,12\}\ \langle 2\,\bar{4}\,1\rangle$, $\{\bar{1}\,1\,7\}\ \langle 2\,\bar{4}\,1\rangle$ and $\{\bar{1}\,0\,6\}\ \langle 2\,\bar{4}\,1\rangle$ (with the RD in common), in addition to the primary density tube described in Table I.

References

1. C. S. CHOI and H. J. PRASK, *J. Appl. Crystallogr.* **18** (1985) 141.
2. G. Y. CHIN, in "Metals Handbook", Vol. 8 edited by T. Lyman (American Society for Metals, Metals Park, OH, 1973) p. 232.
3. C. S. CHOI, H. J. PRASK and S. F. TREVINO, *J. Appl. Crystallogr.* **12** (1979) 327.
4. J. S. KALLEND, U. F. KOCKS, A. D. ROLLETT, and H.-R. WENK, *Mater. Sci. Eng.* **A132** (1991) 1.
5. S. MATTHIES, H. R. WENK and G. W. VINEL, *J. Appl. Crystallogr.* **21** (1988) 285.
6. H. J. BUNGE, "Texture Analysis in Materials Science. Mathematical Methods", translated by P. R. Morris (Butterworths, London, 1982).
7. U. F. KOCKS in "Eighth International Conference on Textures of Materials", edited by J. S. Kallend and G. Gottstein (Metalurgical Society, Warrendale, PA, 1988) p. 31.
8. C. S. CHOI, E. F. BAKER and J. OROSZ, "Advances in X-Ray Analysis", Vol. 37, edited by J. V. Gilfrich, C. C. Goldsmith, T. C. Huang, R. Jenkim, I. C. Noyan, D. K. Smith and P. K. Predecki (Plenum Press, New York, 1994) pp. 49–57.

Received 20 September 1995
and accepted 15 January 1996